

Supplementary Information

Influence of the supramolecular design on the electrical properties of coordination polymers based materials

Chiara Musumeci,^a Silvio Osella,^b Laura Ferlauto,^{a,d} Dorota Niedzialek,^b Luca Grisanti,^b Sara Bonacchi,^a Abdelaziz Jouaiti,^c Silvia Milita,^d Artur Ciesielski,^a David Beljonne,^b Mir Wais Hosseini,^c Paolo Samorì.^a

^aISIS & icFRC, Université de Strasbourg & CNRS, 8 allée Gaspard Monge, 67000, Strasbourg, France. E-mail: samori@unistra.fr

^b Laboratory for Chemistry of Novel Materials, University of Mons, Place du Parc 20, B-7000 Mons, Belgium. E-mail: david.beljonne@umons.ac.be

^cLaboratoire de Chimie de Coordination Organique, UMR CNRS 7140, Université de Strasbourg, 4 rue Blaise Pascal, 67000 Strasbourg, France. E-mail: hosseini@unistra.fr

^dCNR - Istituto per la Microelettronica e Microsistemi (IMM), via Piero Gobetti 101, I-40129 Bologna, Italy

Contents

1. Optical microscopy of (CoTAP) _n and (PdTAP) _n thin films	SI-2
2. Photophysical characterization	SI-2
3. GIXRD analysis of the (CoTAP) _n and (PdTAP) _n films	SI-5
4. Molecular packing simulations of the (PdTAP) _n film	SI-5
5. Electrical characterization at the nanoscale	SI-9
6. Interchain charge transport abilities of the (PdTAP) _n polymer	SI-9

1. Optical microscopy of CoTAP and PdTAP thin films

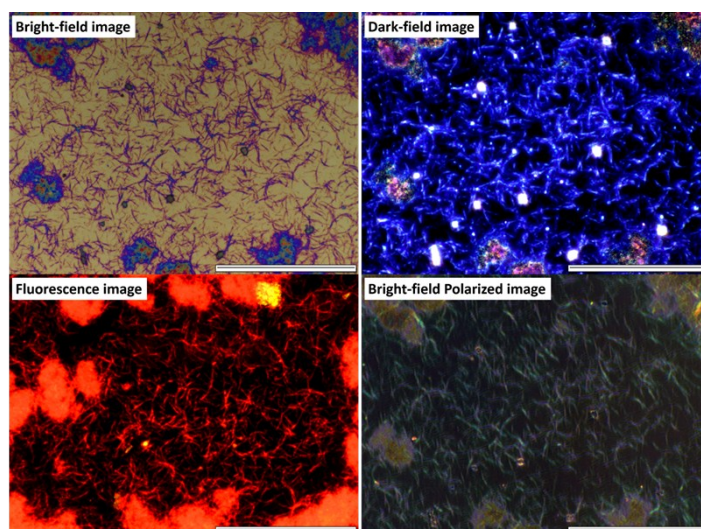


Figure S1. Optical micrographs of (PdTAP)_n. (scale bar, 40 μm)

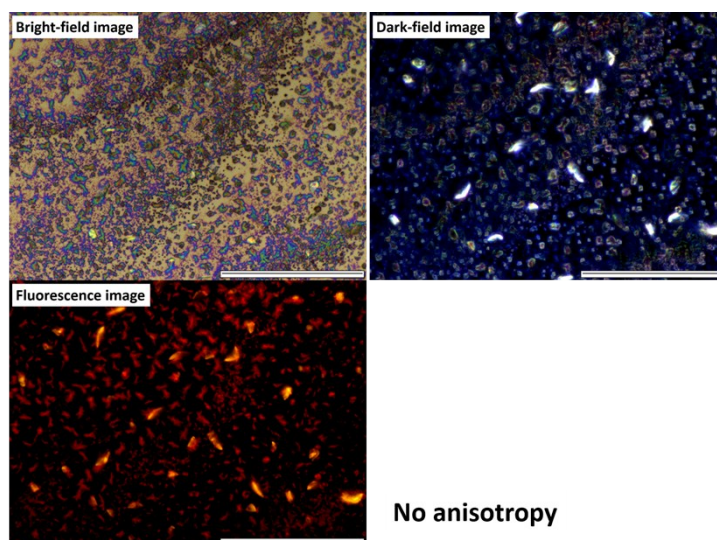


Figure S2. Optical micrographs of (CoTAP)_n (scale bar, 40 μm).

2. Photophysical characterization

The complexation of TAP ligand with CoCl₂ and Pd(OAc)₂ was studied by UV-Vis titration. The UV-vis spectra of TAP ligand (Figure S3) in chloroform (CHCl₃) revealed the characteristic vibrational band of anthracene in the visible region (440 and 470 nm) and a broad and unstructured band around 300 nm that can be attributed to the terpyridine moiety; the pyridine band in UV region is hidden by the higher intense peak of anthracene at 270 nm. Interesting, due to the high conjugation among the free moieties (i.e. anthracene, pyridine and

terpyridine units) in the TPA ligand, the anthracene vibrational bands are less resolved and red-shifted than the relative dye in solution. Moreover, the TPA ligand exhibits intense fluorescence centred around 500 nm.

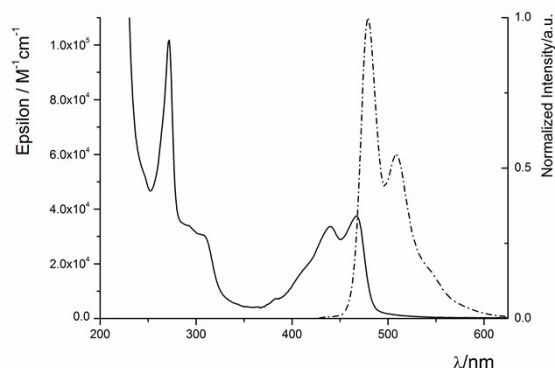


Figure S3. Absorption (solid line) and emission ($\lambda_{\text{exc}} = 390 \text{ nm}$; dashed line) spectra of the TAP ligand in acetonitrile.

For both the metal ions, distinct changes in TAP absorption were observed upon complexation (Figure S4). As expected, complexation induces an increase in absorbance between 300 and 350 nm and a decrease at wavelengths below 300 nm, corresponding to the change in terpyridine absorption. Moreover, both the complexes show new intense absorption in the visible region ($\lambda > 500 \text{ nm}$) due to the increase of the conjugation of the TAP ligand upon the complexation. Interesting, clear isosbestic points were found only for $(\text{PdTAP})_n$ indicating that only this metal ion a single equilibrium between two species, i.e. free and complexed TAP, occurs during the titration. The fluorescence of anthracene chromophore inside TAP is drastically quenched upon addition of both the metal ions (Figure S5), which could be due to intramolecular electron-transfer from the metal complex to the anthracene unit.

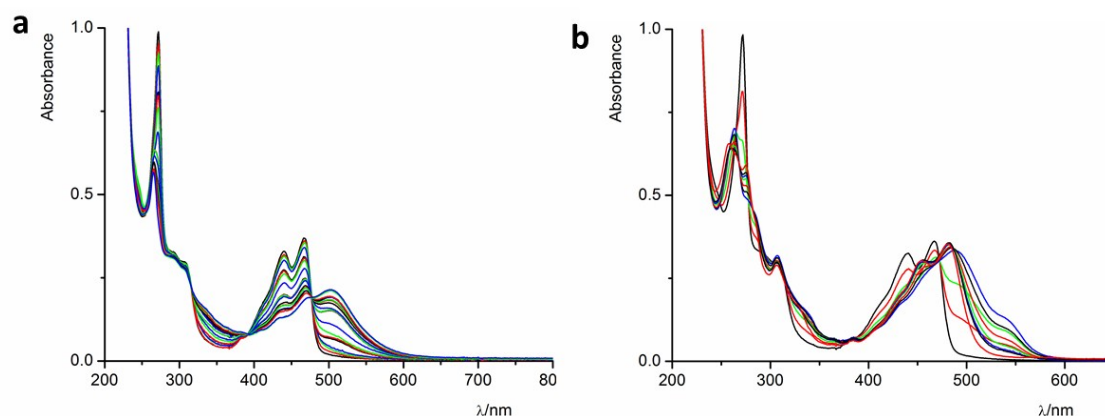


Figure S4. UV-Vis titrations of TAP ($C = 1 \times 10^{-5} \text{ M}$) with (a) Pd(II) and (b) Co(II) in CHCl_3 up to 1 equivalent of metal ions.

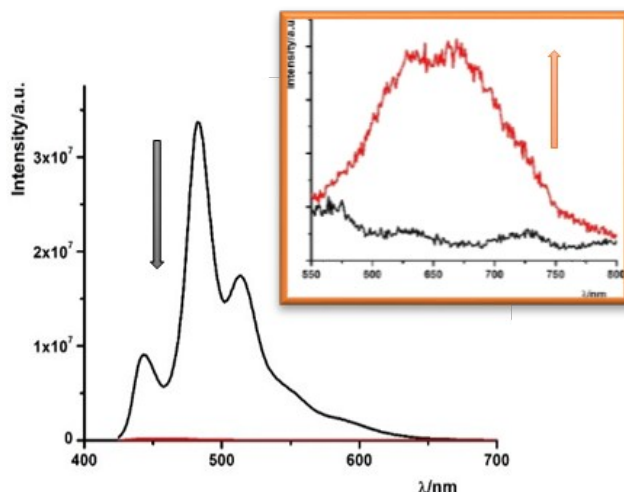


Figure S5. Quenching of luminescence of TAP ($\lambda_{\text{exc}} = 390 \text{ nm}$) after the addition of 1 equivalent of $\text{Pd}(\text{OAc})_2$.

With the aim of elucidate the supramolecular polymer formation, solutions at different concentrations of complexed TAP (1:1 stoichiometry) were studied (Figure S6). In particular, increasing the concentration from $1 \times 10^{-5} \text{ M}$ to $5 \times 10^{-4} \text{ M}$ of the $(\text{PdTPA})_n$ complex, the red-shifted band at $\lambda > 500 \text{ nm}$ became more and more broad and red-shifted, which could be ascribed to the formation of high conjugated aggregates among the anthracene moiety, in agreement with AFM and XRD results. Interestingly, it was not possible to perform the same kind of experiment in the case of CoCl_2 due to the formation, immediately after the addition of 1 equivalent of metal, of brownish and insoluble aggregates in solution.

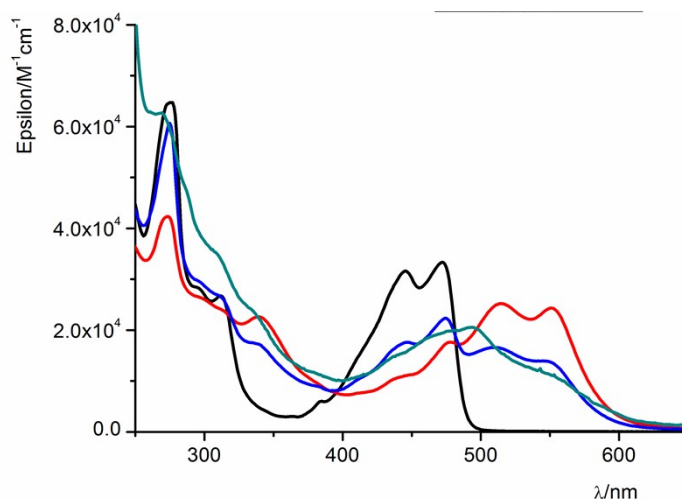


Figure S6. Absorption spectra of TAP (black line) + $\text{Pd}(\text{II})$ in an equimolar mixture, at $1 \times 10^{-5} \text{ M}$ (green line, $b = 10 \text{ mm}$); at $1 \times 10^{-4} \text{ M}$ (blue line, $b = 2 \text{ mm}$) and at $5 \times 10^{-4} \text{ M}$ (red line, $b = 1 \text{ mm}$), recorded in CHCl_3 at room temperature, showing the formation of a new structured red shifted band.

3. GIXRD analysis of the (CoTAP)_n and (PdTAP)_n films

Table S1: Average crystalline domains size (D) of the (CoTAP)_n film, calculated estimated from the full width at half maximum (FWHM) along the three crystallographic directions of the peaks (Δq) of Figure 2b by using the Sherrer equation ($D = 2\pi K/\Delta q$, where $K \approx 0.9$)

Peak	Δq (\AA^{-1})	D (\AA)
1	0.027	209
2	0.021	269
3	0.040	141
4	0.060	94

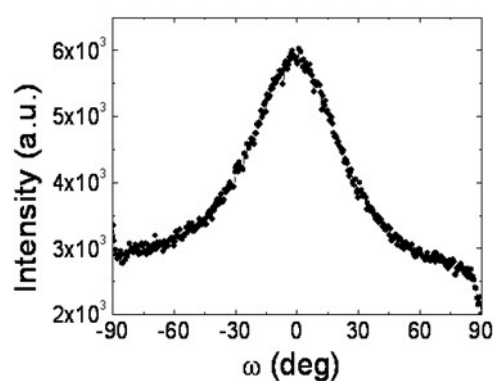


Figure S7: Radial integration of the 2D-GIXRD image for the (CoTAP)_n film from which the average degree of misorientation was estimated to be $\sim 50^\circ$.

4. Molecular packing simulations of the PdTAP film

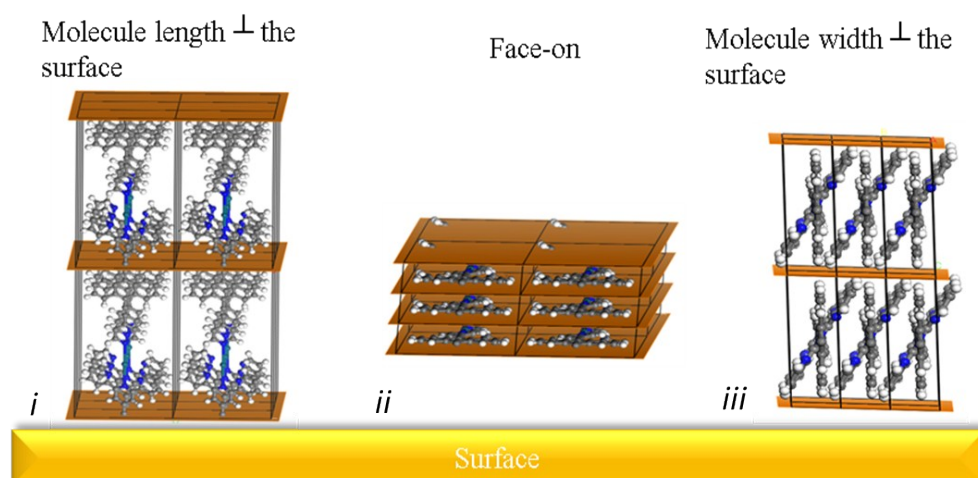


Figure S8. Three possible orientations of the polymer on the surface considered in the calculations. The orange planes refer to the Miller planes.

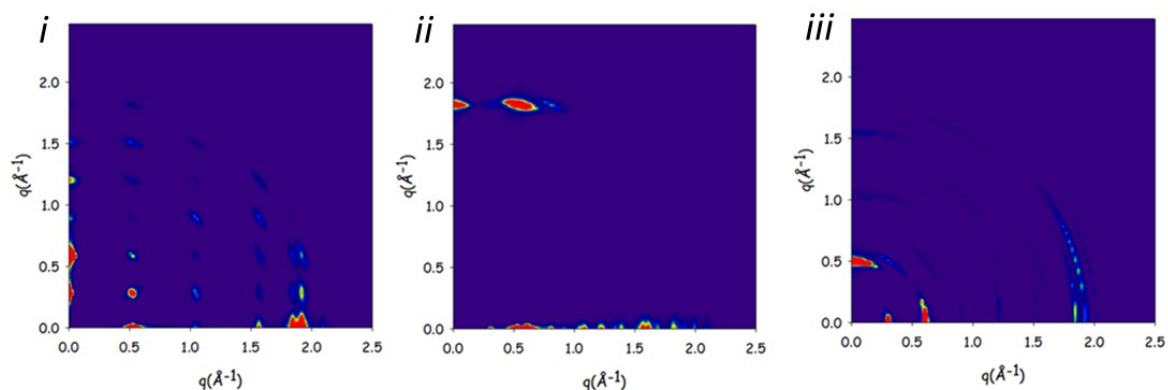


Figure S9. Simulated GIXRD patterns for each of the three orientations presented in Figure S8: with (i) along molecule axis oriented perpendicular to the surface, (ii) polymer plane-on and (iii) edge-on orientation with respect to the surface, respectively.

To study the effect of the torsion on the bandgap energy, three different cases were considered. In the first analysis, the terpyridine and pyridine groups are forced to be planar; in the second the terpyridine and the anthracene units are planarized and the third analysis concerns the full planarization of the three groups. The three structures differ in energy by up to 0.28 eV from the optimized polymer. The resulting bandgap are reported in Figure S10.

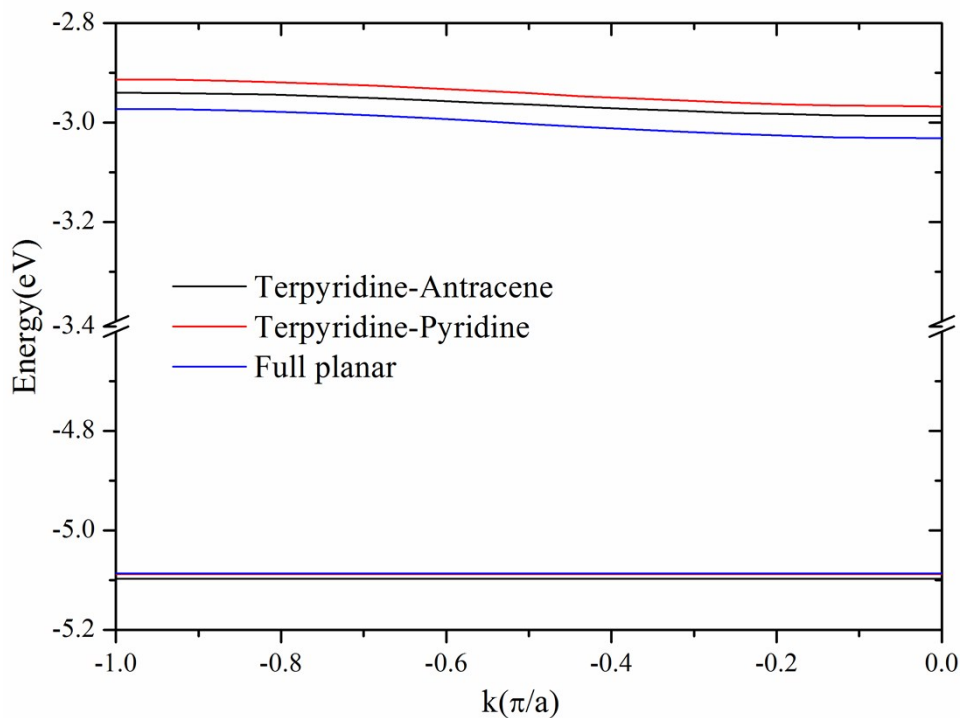


Figure S10. Band structure analysis of the polymer with different degree of planarization between terpyridine, anthracene and pyridine groups.

In all three cases, the different planarization of the structures does not affect the HOMO energy, lying now at -5.10 eV with a destabilization of only 0.07 eV. On the other hand, the different degrees of torsion have a slight impact on the LUMO energy, with a stabilization by up to 0.17 eV for the full planar system. As consequence, the bandgap of the polymer only slightly change, going from 2.05 eV when he three units are fully planar, to 2.12 eV for the planarization of the terpyridine-pyridine and terpyridine-antracene units (to be compared with a bandgap of 2.30 eV obtained after optimization). A similar behavior is found for the bandwidth analysis: while the valence band (VB) width is flat in all cases the conductive band (CB) width increased up to 0.06 eV for the fully planar system (to be compared with a bandwidth of 0.05 eV obtained after optimization). Hence, the full planarization of the different units of the polymer only slightly affects the electronic properties of the system.

Pyridine torsion degree	HOMO	LUMO
0		
10		
20		
30		
40		

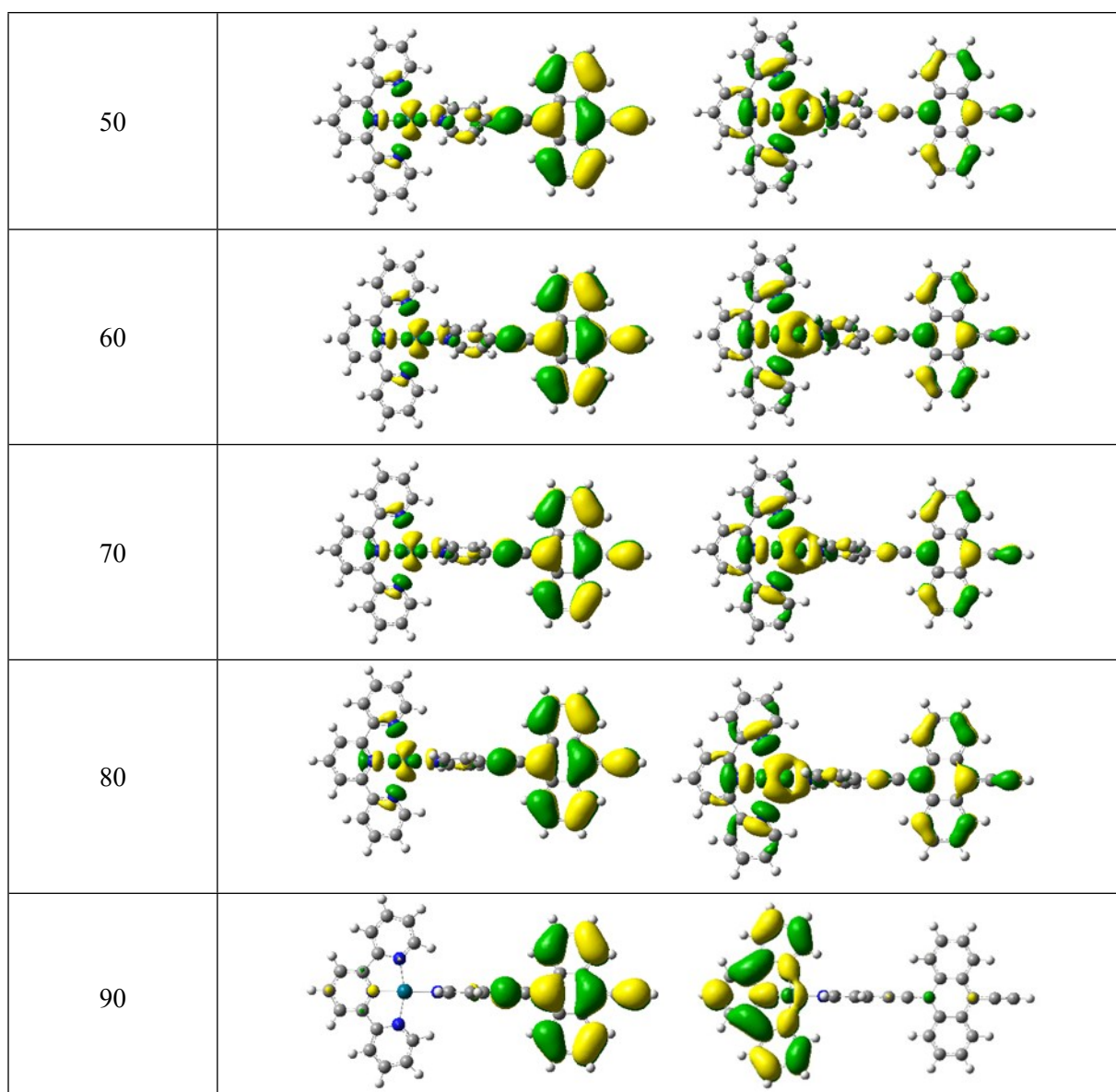


Figure S11. Differences in localization of the frontier orbital of the monomer while increasing the torsion of the pyridine ring from planarity to 90 degrees.

5. Electrical characterization at the nanoscale

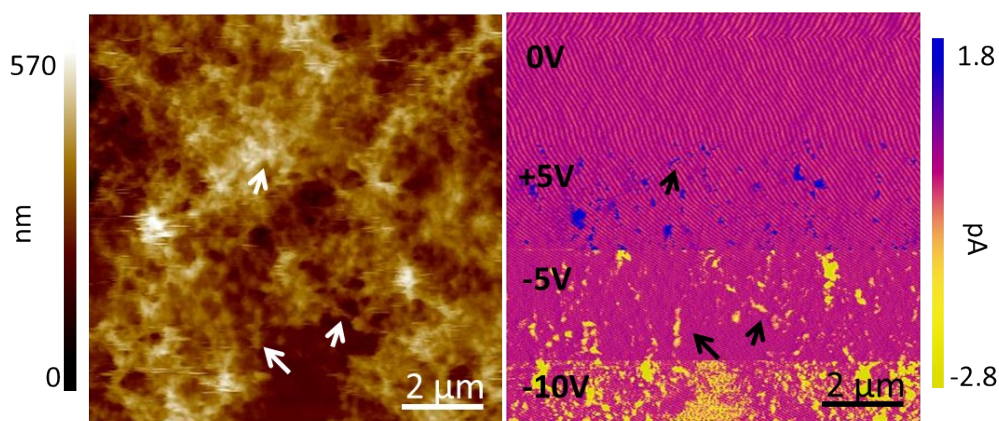


Figure S12: C-AFM topography and current map images of a network of molecular wires of $(\text{PdTAP})_n$ on a gold electrode. In the current map four different areas are visible corresponding to 0, +5, -5 and -10V applied on the gold bottom electrode. The arrows highlight fiber structures in the film.

6. Interchain charge transport abilities of the PdTAP polymer

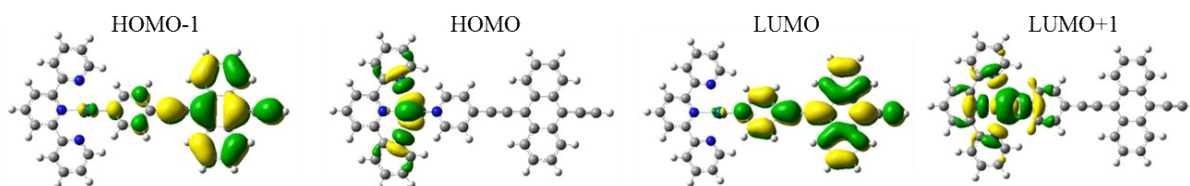


Figure S13. Shape of the frontier molecular orbitals for the monomer with the application of two point charges perpendicular to the square planar coordination plane and at a distance of 2 Å from the metal center.